



**HAL**  
open science

**Identification and quantification of domoic acid by  
UHPLC/QTOF tandem mass spectrometry, with  
simultaneous identification of non-target  
photodegradation products**

Anne-Laure Gagez, Antoine Bonnet, Philippe Pineau, Marianne Graber

► **To cite this version:**

Anne-Laure Gagez, Antoine Bonnet, Philippe Pineau, Marianne Graber. Identification and quantification of domoic acid by UHPLC/QTOF tandem mass spectrometry, with simultaneous identification of non-target photodegradation products. *International Journal of Environmental Analytical Chemistry*, 2017, pp.1 - 14. 10.1080/03067319.2017.1393538 . hal-01630105

**HAL Id: hal-01630105**

**<https://hal.science/hal-01630105>**

Submitted on 15 Jan 2018

**HAL** is a multi-disciplinary open access archive for the deposit and dissemination of scientific research documents, whether they are published or not. The documents may come from teaching and research institutions in France or abroad, or from public or private research centers.

L'archive ouverte pluridisciplinaire **HAL**, est destinée au dépôt et à la diffusion de documents scientifiques de niveau recherche, publiés ou non, émanant des établissements d'enseignement et de recherche français ou étrangers, des laboratoires publics ou privés.

1 **Identification and quantification of domoic acid by UHPLC/QTOF tandem mass**  
2 **spectrometry, with simultaneous identification of non-target photodegradation**  
3 **products**

4

5

6 Anne-Laure Gagez<sup>1</sup>, Antoine Bonnet<sup>1</sup>, Philippe Pineau<sup>1</sup> and Marianne Graber<sup>1</sup>

7

8 <sup>1</sup> UMR CNRS 7266 LIENSs, Université of La Rochelle, Bâtiment Marie Curie, Avenue Michel  
9 Crépeau, 17042 La Rochelle, France.

10

11 Dr. Anne-Laure Gagez: [anne-laure.gagez@univ-lr.fr](mailto:anne-laure.gagez@univ-lr.fr)

12 Antoine Bonnet: [antoine.bonnet@univ-lr.fr](mailto:antoine.bonnet@univ-lr.fr)

13 Philippe Pineau: [philippe.pineau@univ-lr.fr](mailto:philippe.pineau@univ-lr.fr)

14 Pr. Marianne Graber: [mgraber@univ-lr.fr](mailto:mgraber@univ-lr.fr)

15

16 Corresponding author:

17 Pr. Marianne Graber

18 UMR CNRS 7266 LIENSs, Bâtiment Marie Curie

19 Avenue Michel Crépeau

20 17042 La Rochelle

21 France

22 [mgraber@univ-lr.fr](mailto:mgraber@univ-lr.fr)

23 phone: +33 5 46 45 86 30

24 fax: +33 5 46 45 82 65

25 Abstract

26 Amnesic shellfish poisoning is a potentially lethal human toxic syndrome which is caused by  
27 domoic acid (DA), a neurotoxin produced by marine phytoplankton, principally from  
28 *Pseudonitzschia* genus. In this report, a method to identify and quantify the DA toxin, with  
29 simultaneous identification of its photodegradation products has been developed. It uses an Ultra  
30 High Performance Liquid Chromatography coupled to a Quadrupole-Time-Of-Flight tandem mass  
31 spectrometer (UHPLC-QTOF) after solid-phase extraction. An unambiguous identification of DA  
32 was carried out by considering both the retention time of DA in UHPLC and the exact mass of  
33 protonated DA molecule ( $[M+H]^+ = 312.1447$  m/z) and of the most intense fragment ion (m/z  
34 266.1391). The quantification was conducted using protonated DA molecule with protonated  
35 Glafenin as internal standard, obtaining a LOD of  $0.75 \mu\text{g L}^{-1}$ . Large screening with UHPLC-  
36 QTOF could also give structural informations about degradation products of DA present in samples  
37 after UV-irradiation. This method was applied for the determination of DA in complex liquid  
38 samples after solid-phase extraction, and is applicable for environmental monitoring of this toxic  
39 substance in the aquatic environment.

40

41

42 Keywords: Domoic Acid, Toxin, Seawater, Liquid chromatography, Mass spectrometry, Accurate  
43 mass

44

## 45 1. Introduction

46 Domoic acid (DA) was identified as a marine neurotoxin at the end of the 1980s following human  
47 poisoning incident in Canada, after consumption of cultured blue mussels *Mytilus edulis* [1]. Red  
48 algae and diatoms were found to be primary producers of DA [2], but it is the accumulation of DA  
49 in filter-feeding marine organisms which poses the biggest threat to human health. Symptoms  
50 produced by this algal toxin include, among other clinical signs, in many of the seriously  
51 intoxicated individuals, persistent short term memory loss. The syndrome was thus called amnesic  
52 shellfish poisoning (ASP) [3]. DA intoxication in wild animals, such as anchovies, sea lions,  
53 whales, sea birds and fishes, has been reported [2, 4-7]. DA is a water soluble, polar, non-protein  
54 amino acid, whose chemical structure was determined by NMR [2] and then confirmed following  
55 total synthesis [8]. It consists of a proline ring, three carboxyl groups and an imino group, which  
56 leads to four chargeable groups that can exist in up to five charged states from  
57 -3 to 1 depending on the pH (Figure 1). At room temperature, DA is relatively stable and does not  
58 degrade [9]. At neutral pH, DA has an absorption maximum of 242 nm due to its conjugated diene  
59 moiety [5]. DA elimination in the marine environment is essentially by photodegradation *via*  
60 sunlight mediated reactions [10]. DA has at least nine geometrical isomers. Among them isodomoic  
61 acids D, E and F and the 5'-epi-domoic acid have been isolated from plankton cells and shellfish  
62 tissue and have been found to be less toxic than DA [11].

63 To protect human health and seafood safety, the European Union has established that total DA  
64 content must not exceed 20µg DA/g in the edible parts of molluscs [12]. This limit is employed  
65 worldwide for harvesting and consumption of shellfish resources to protect human health [13].  
66 Numerous liquid chromatographic methods with ultraviolet diode array detection (HPLC-UVD) can  
67 be used following extraction of DA from homogenised tissue by solvent and SPE (solid phase  
68 extraction) clean-up [14]. The diene chromophore of DA permits its detection by HPLC-UVD at  
69 concentrations as low as 4–80 µg L<sup>-1</sup> depending on the sensitivity of the detector [15]. To further  
70 decrease the LOD, liquid chromatography with fluorimetric detection methodologies (HPLC-FLD)

71 after derivatisation has been developed in research laboratories for monitoring DA in seafood and  
72 marine phytoplankton [13]. Indeed a laboratory culture of diatom genus *Pseudonitschia* produces  
73 DA at levels ranging from 1 to 20 pg/cell, with less than  $1 \mu\text{g L}^{-1}$  found in the culture medium [16].  
74 In both HPLC-UVD and HPLC-FLD methods, DA is identified based on the coincidence of LC  
75 retention time of the suspected chromatographic peaks, with those of DA standard peaks; however,  
76 the suspected toxin peaks may represent compounds other than DA. An unambiguous method such  
77 as LC–mass spectrometry (LC–MS) must be used to confirm the presence of DA, especially for  
78 newly suspected source organisms or for confirming the appearance of DA in a new geographical  
79 region. So, even if HPLC-UV methods is often the only analytical tool available in many research  
80 institutes and regulatory agencies responsible for monitoring the occurrence of DA, many mass  
81 spectrometry methods were developed in different research laboratories [14,17, 18, 19].  
82 Moreover for researchers, the development of very sensitive methods to determine DA in seawater  
83 is still a challenge. Indeed the role of dissolved DA in seawater, its distribution patterns across the  
84 trophic webs and its production by minimally toxic phytoplankton species are not fully understood.  
85 This study describes a method for unequivocal confirmation of DA and its quantitative analysis in  
86 seawater and in complex liquid media by using ultra high performance liquid chromatography  
87 coupled to quadrupole-orthogonal time-of-flight tandem mass spectrometer (UHPLC- QTOF),  
88 Xevo G2 QToF MS (Waters, Milford, USA), with an electrospray ionization (ESI). Assalts  
89 adversely affect ESI performance by making ion formation less reproducible, a SPE method was  
90 developed to simultaneously extract DA and remove salts from samples. Conditions affecting the  
91 stability of DA were also investigated. The  $\text{MS}^E$  data collection technique was used, which allows  
92 to obtain fragmentation information for all compounds in a single run. Indeed two separate  
93 acquisition functions are sequentially measured in full scan mode: one for MS of precursors  
94 acquired at low collision cell energy and one for collecting fragmentation data at elevated collision  
95 cell energies. The correlation of product to precursor ions is achieved, after deconvolution, by using  
96 reconstructed retention time apices and chromatographic peak shapes. In the present case, as

97 fragmentation information is obtained in advance for all compounds in a single run, it was possible  
98 to simultaneously quantify DA and identify non-target degradation products of DA after UV-  
99 irradiation in a single run. This UV treatment was performed in order to simulate *in vitro* natural sun  
100 degradation of DA. This constitutes a real novelty, offered by the possibility of performing  
101 retrospective full data examination, without re-injecting sample.

102

## 103 2. Experimental

### 104 2.1. Chemicals and Reagents

105 Domoic acid (DA) (powder form stored at -20°C) and formic acid (FA) were purchased from VWR  
106 International LLC (Radnor, PA, USA). Leibovitz's L-15 medium and fetal bovine serum (FBS,  
107 S1520-500) were from Sigma (Steinheim, Germany).

108

### 109 2.2. Extraction of DA from liquid samples by SPE

110 Oasis® HLB, Hydrophilic-Lipophilic-Balanced, 1 cc Vac Cartridge, 30 mg Sorbent per Cartridge  
111 (Waters, Milford, USA) was used for extraction. The choice of this cartridge was also based on pH  
112 stability from 0 to 14, absence of silanol interactions, and large use for acid, base and neutral  
113 compounds extraction. Leibovitz's L-15 culture medium, which contains many amino acids,  
114 vitamins and salts, supplemented with 10% (v/v) foetal bovine serum was used as complex liquid  
115 medium, to optimize SPE step. Samples were first spiked with 200 µg L<sup>-1</sup> of DA, then acidified  
116 with 2% FA, vortex-mixed, centrifuged 10 min at 10,000 g and submitted to SPE. No vacuum was  
117 applied during sample loading to ensure optimal binding of DA on sorbent. During following steps  
118 of extraction, the vacuum was kept approximately at -17kPa. An optimized HLB cartridge protocol  
119 was applied as follows: the cartridge was first conditioned with 1mL of methanol (MeOH) and 1mL  
120 of water containing 2% FA. Afterwards, 1mL of sample previously acidified with 2% of FA was  
121 loaded and washed with 1 mL of H<sub>2</sub>O. Finally, DA was eluted with 1mL of MeOH:H<sub>2</sub>O (40:60, v/v)  
122 with 2% FA. Then 85 µL of the eluate were transferred to ultra high performance liquid

123 chromatography (UHPLC) vials containing 15  $\mu\text{L}$  of Glafenin (GLF) (5 mg/L) as the internal  
124 standard (IS). To investigate the efficiency of the SPE method for DA, RE (Recovery of the  
125 Extraction) was determined by comparing the mean peak areas of replicate analyses (n=5) of DA  
126 quantification (ratio of DA to IS) obtained before and after SPE extraction (DA spiked at 200  $\mu\text{g L}^{-1}$ ),  
127 as described by Matuszewski [20]. Assessment of ME (Matrix Effect) was realized by  
128 comparing the mean peak area of replicate analyses (n=5) of DA quantification (ratio of DA to IS)  
129 obtained in culture medium spiked with DA and IS after SPE extraction and in neat solution  
130 standards, as described by Matuszewski [20].

### 131 2.3. Salinity measurement

132 Artificial seawater (33 g/L) was prepared with ready-to-use sea salt containing all 70 trace elements  
133 found in natural seawater (Tropic Marin<sup>®</sup>, Wartenberg, Germany). One part of this artificial  
134 seawater solution was spiked with DA (final concentration 340  $\mu\text{g L}^{-1}$ ) to constitute the sample, and  
135 the other part constituted the control. SPE was performed such as previously described in paragraph  
136 2.2 with salvage of each liquid fraction getting through the SPE cartridge.

137 Salinity and temperature were measured by a conductivity meter Cond 3110 with standard  
138 conductivity measuring cell TetraCon 325 (WTW, Germany). Conductivity measuring cell was  
139 immersed in a tube with 7 ml of replicate and after 1 minute for stabilization.

140

### 141 2.4. Photodegradation of DA

142 Photodegradation of DA was obtained by irradiating a solution of 340  $\mu\text{g L}^{-1}$  DA in artificial sea  
143 water, in glass container without lid with UV radiation at 254 nm, 6 W, 710  $\mu\text{W}/\text{cm}^2$ . The UV lamp  
144 was from Vilber Lourmat (Torcy, France). The irradiation experiments were conducted for 3 h with  
145 the control sample kept in the dark.

146

### 147 2.5. UHPLC-MS/MS Method

148 Analyses were performed using an Acquity UPLC H-Class (Waters, Milford, USA) coupled to a

149 Xevo G2 S Q-TOF mass spectrometer equipped with an electrospray ionization (ESI) source. The  
150 chromatographic system consisted of a quaternary pump (Quaternary Solvent Manager) and an  
151 autosampler (Sample Manager-FTN) equipped with a 10  $\mu\text{L}$  sample loop. 5  $\mu\text{L}$  of the sample was  
152 injected into a Waters Acquity UPLC BEH C18 column (2.1 x 50 mm, 1.7  $\mu\text{m}$ ). The system was  
153 operated under the following gradient elution program: solution A (0.01% FA in  $\text{H}_2\text{O}$ ) in solution B  
154 (0.01% FA in MeOH) at a flow rate of 300  $\mu\text{L}/\text{min}$  as follows: 0-0.2 min, 3% B; 0.2-0.25 min, 3-  
155 20% B; 0.25-1 min, 20-55% B; 1-1.5 min, 55-100% B; 1.5-3.5 min, 100% B; 3.5-3.6 min, 100-3%  
156 B; 3.6-4.5 min, 3%B. The column and the autosampler were maintained respectively at +25°C and  
157 +7°C.

158 ESI was shown as the optimum ion source interface for DA analysis [21]. Optimization of mass  
159 spectrometry parameters was performed in two steps: first, by direct infusion of DA at constant flow  
160 of 20  $\mu\text{L min}^{-1}$  and second, by infusion combined with liquid chromatography flow equal to 50 $\mu\text{L}$   
161  $\text{min}^{-1}$ . Final ESI conditions were: source temperature 120°C, desolvation temperature 500°C, cone  
162 gas flow 50  $\text{L h}^{-1}$ , desolvation gas flow 1000  $\text{L h}^{-1}$ , capillary voltage 2.5 kV, sampling cone 35 and  
163 source offset 80. The instrument was set to acquire over the  $m/z$  range 50-1200 with a scan time  
164 equal to 0.15 s. These conditions gave a resolution equal to 30000 for protonated DA molecule  
165 ( $[\text{M}+\text{H}]^+ = 312.1447 \text{ m/z}$ . Data were collected in the positive (ESI+) electrospray ionization modes.  
166 The MS and the MS/MS experiments were performed using the  $\text{MS}^E$  function in centroid mode. A  
167  $\text{MS}^E$  approach consists in MS and MS/MS data acquisitions in a single same run, with no collision  
168 energy in function 1 (MS experiment) and a collision energy ramp of 15-45 V in function 2  
169 (MS/MS experiment). Leucine Enkephalin ( $[\text{M}+\text{H}]^+ = 556.2771 \text{ m/z}$ ) ( $1 \text{ ng } \mu\text{L}^{-1}$ ) was used as lock  
170 mass for mass shift correction. The mass spectrometer was calibrated before analyses using 0.5mM  
171 sodium formate solution.

172 DA quantitation was obtained by calibration curve of DA standard reference at the following  
173 concentrations: 2.5, 5, 10, 25, 50, 100, 250, 500, 1000 $\mu\text{g L}^{-1}$ , prepared by cascade dilution in  
174 MeOH:H<sub>2</sub>O (40:60, v/v) with 2% FA before each run. After vortex-mixing, 85  $\mu\text{L}$  of each standard



175 was transferred to UHPLC vials containing 15  $\mu\text{L}$  of GLF ( $5 \text{ mg L}^{-1}$ ) as internal standard.

176

## 177 2.6. Analytical validation

178 Intraassay precision was studied by preparing and analysing five independent replicates of DA  
179 quality controls prepared as described above at different concentrations (20, 40, 80, 200, 400, and  
180  $800 \mu\text{g L}^{-1}$ ) on a given day. Interassay precision and linearity were evaluated from the analysis of a  
181 calibration set each day during 5 days.

182 To evaluate the stability of DA in MeOH:H<sub>2</sub>O (40:60, v/v) with 2% FA, that correspond to the  
183 injection conditions of DA, extraction of DA was performed as described in 2.2. One aliquot of  
184 elution was analysed immediately. Four aliquots of the same sample supernatant were kept at +7°C  
185 in the autosampler for 6 h and 22 h, at +4°C in a refrigerator for 4 days and 15 days and at -20°C in  
186 a deep-freeze for 24 h prior to analysis. A sixth aliquot was used to study the stability of DA over  
187 three freeze (-20°C)-thaw (room temperature) cycles. Three replicates of each aliquot were analysed  
188 and compared with independently and extemporaneously prepared calibration curves with DA in  
189 powder form stored at -20°C. The mean concentration of DA immediately analysed in triplicate was  
190 used as control for comparison with other samples.

191

## 192 2.7. Data analysis

193 Post-acquisition analyses were performed using the MassLynx™ V4.1 program (Waters, Milford,  
194 USA). Using ChromaLynx™ application, compounds were first identified based on their retention  
195 time, mass accuracy and fragment confirmation. Then, positively identified compounds in each  
196 sample were transferred to quantification using the software TargetLynx™. The MetaboLynx™  
197 application automates the process of peak detection, comparison of data between DA control sample  
198 and DA sample after photodegradation and also for filtering the matrix-related peaks. Peaks only  
199 present in DA sample after photodegradation are considered as molecules produced by  
200 transformation of parent. MetaboLynx™ software used elemental composition to suggest formula

201 of degradation products. Elemental composition parameters were: 5 ppm mass tolerance, with 0 to  
202 50 for the number of carbon atoms, from 0 to 100 for the number of hydrogen atoms, from 0 to 20  
203 for the number of nitrogen atoms, from 0 to 20 for the number of oxygen atoms and from 0 to 1 for  
204 the number of sodium atoms.

205

### 206 3. Results and discussion

207

#### 208 3.1. Fragmentation of DA standard

209 Ionization of DA was better in positive mode than in negative mode and MS conditions were  
210 optimized (see detailed values in 2.3 “Material and methods”). DA identification was confirmed by  
211 MS and MS/MS fragmentation patterns (Fig. 2). Full mass spectra from DA standard shows the  
212 major molecular ion for the toxin at  $m/z$  312.1447  $[M+H]^+$ , and a peak at  $m/z$  334.1263 is attributed  
213 to the  $[M+Na]^+$  sodium adduct ion. The fragmentation profile produced in high collision energy  
214 function consists mainly in water ( $H_2O$ ), formic acid ( $CH_2O_2$ ) and CO losses (Fig. 2). Table 1  
215 displays elemental composition, corresponding fragmentation or adduct ion, theoretical mass,  
216 measured mass and mass errors in ppm of reference DA and its major fragment ions. The maximum  
217 mass errors between theoretical and observed values were less than 5 ppm, which means high  
218 resolution and good accuracy of measures by theselected method.

219 Exact mass of the fragmentation of the  $[M+H]^+$  adduct ion of DA is detailed in Table 1 and Fig. 2B.

220 The most intense fragment ion ( $m/z$  266.1391) of DA is due to the loss of a  $H_2O$  molecule (18 Da).

221 Based on this information, the different fragmentation pathways of DA are proposed in Fig. 3.

222 Results obtained by exact mass measurements coincide with those reported by other authors using  
223 single quadrupole [22], ion-trap single quadrupole [17,23,24], or triple quadrupole with [13,15,25]  
224 or without trap technology [21] mass spectrometer.

225

#### 226 3.2. UHPLC method optimisation of DA

227 Efficient separation of DA and GLF from impurities was performed in 4.5 minutes. Peaks of DA  
228 and GLF were in the middle of the chromatogram, with retention times respectively equal to 2.22  
229 and 2.39 min (Fig.4) Column temperature was tested, from +25°C to +80°C, with a step of +5°C. No  
230 significant difference in DA quantification was observed, except at +80°C where the analyte started  
231 to be degraded (data not shown).

232 In several previous studies the column temperature chosen for liquid chromatographic separation  
233 was between +40°C and +70°C [13,15,21,25] but with our system, heating the column above 25°C  
234 did not increase the detection nor the quantification limits of DA. The temperature of +25°C was  
235 thus adopted.

236 Mass spectrometer parameters were first optimized by injecting standard reference solution of DA  
237 in infusion mode and finalized in combined mode, namely by using a combination of infusion mode  
238 with an UHPLC flux (0.05 mL/min.). Generally, for small molecules, the best tension capillary is  
239 0.5 kV in combined mode, but for DA detection, better response was obtained with 2.5 kV, close to  
240 value used in infusion mode, 3 kV. DA identification was possible in both positive and negative  
241 mode, but positive mode was more sensitive.

242 DA was identified from MS<sup>E</sup> acquisition data by together its retention time (2.22 min.), its mass  
243 accuracy given by the elemental composition (C<sub>15</sub>H<sub>21</sub>NO<sub>6</sub><sup>+</sup>) and one chosen fragment (m/z  
244 266.1392) corresponding to elemental composition C<sub>14</sub>H<sub>20</sub>NO<sub>4</sub><sup>+</sup> to confirm the presence of the  
245 molecule. For GLF identification, both retention time (2.39 min.) and mass accuracy  
246 (C<sub>19</sub>H<sub>18</sub>N<sub>2</sub>O<sub>4</sub>Cl<sup>+</sup>): [M+H]<sup>+</sup>= 373.0955 m/z were used. Integration parameters were optimized and  
247 mean function was chosen as smoothing method. It consists in taking the arithmetical mean of the  
248 intensities of the data points in each window along the chromatogram. Identified analytes were  
249 quantified using GLF as internal standard.

250

### 251 3.3. Extraction of DA from liquid samples by SPE

252 According to the HLB generic method, complex liquid samples spiked with DA were acidified

253 before SPE. This allowed a complete retention of DA on the SPE cartridge, while eluting unretained  
254 matrix, with a wash step using 100% water. To finalize the elution step of DA, an optimization  
255 approach was used, using 20 different mixtures as elutant solutions, containing 2% FA or 2%  
256 ammonium hydroxide (AH) in MeOH:H<sub>2</sub>O mixtures with increasing MeOH amounts. MeOH:H<sub>2</sub>O  
257 (40:60, v/v) with 2% FA solution was selected to be the best elutant solution. It was just strong  
258 enough to elute DA while retaining the most hydrophobic interferences on the sorbent. In these  
259 conditions, RE of DA was equal to  $96 \pm 2\%$ , which corresponds to an excellent recovery of DA.  
260 ME was equal to  $95 \pm 2\%$ . This value indicates very slight ionization suppression in the extract  
261 compared to the neat solution.

262

#### 263 3.4. Desalination of sample by solid-phase extraction

264 Removing salt in sample before analysis without loss of the molecules of interest is essential for  
265 subsequent mass spectrometry. The measure of salinity was performed at each step of the solid  
266 phase extraction. The salt concentration in both starting samples (control: artificial sea water and  
267 sample: artificial sea water + 0.34 ng/ $\mu$ L DA) was equal to 28.7 g/L. The salts were recovered  
268 almost entirely in the “load fraction”, respectively at 27.8 and 27.7 g/L, showing that the SPE  
269 cartridge did not retained salts on the column. The salinity of the “wash” and “elution” fractions  
270 were measured with the conductivity meter Cond 3110. They contained respectively salt  
271 concentrations equal to 0.7 and 0.5 g/L, showing that the SPE allowed an almost complete  
272 desalinisation of the samples.

273

#### 274 3.5. Analytical validation

275 Calibration curve obtained using linear regression with a weighting factor of  $1/x^2$  gave regression  
276 correlation coefficients  $R^2=0.994$ . The quantification method showed good intraassay precision,  
277 with mean relative error (MRE) less than 17.4% and relative standard deviation (RSD) always less  
278 than 7.4%. Interassay precision was also good over the concentration range, with MRE inferior to

279 19.3% and RSD inferior to 13.7%.

280 DA compound was found to be stable in its injection solvent (MeOH:H<sub>2</sub>O (40:60, v/v) with 2% FA)  
281 for at least 15 days at +4°C and at least 24 h at -20°C and to tolerate three freeze/thaw cycles, with  
282 maximal deviation from initial time equal to 16.6%, 7.7% and 10.2% respectively . The stability of  
283 DA in the autosampler at +7°C was demonstrated over 22 h, with 2.9% maximal deviation  
284 compared to initial time.

285 The mean signal/noise ratio (S/N) was obtained thanks to software TargetLynx™, by using 10  
286 different blank injections. Limits of detection (LOD) was then estimated on the basis of signal/noise  
287 ratio (S/N) of three, by injecting solutions with lower and lower DA concentrations. LOD was  
288 found to be equal to 0.75 µg L<sup>-1</sup>. This detection limit value, with Q-TOF method was lower than UV  
289 detection (4-80 µg L<sup>-1</sup>, depending on the sensitivity of the detector [15]), because of the sensitivity  
290 and the specificity of the mass detector, and without false positives commonly encountered with UV  
291 method. It was also better than MS single quad or orbitrap detection and was equivalent with the  
292 LOD obtained with triple-quadrupole MS) [26, 27, 28]. Furthermore, the disadvantage of these  
293 SRM or MRM scanning acquisitions is the impossibility to visualize other ions than those isolated  
294 as precursor ion prior to the analysis. In the present case however, with MS<sup>E</sup> data acquisitions used  
295 with Q-TOF, all analytes in sample are detected and saved, including all precursors and their  
296 fragments. This allowed to perform the following additional investigation about DA  
297 photodegradation products, by reprocessing the data, without performing a new sample injection.

### 298 3.6. Identification of DA photodegradation products

299 UV-irradiation of DA induced the appearance of several peaks after extraction at m/z 312.14 ± 0.02  
300 Da (Fig. 5), that potentially corresponded to degradation products of DA. MetaboLynx™ analysis  
301 allowed to identify geometrical isomers of DA based on their measured mass (Table 2, expected  
302 products). Fragmentation pattern of these molecules was then manually confirmed from MS<sup>E</sup> data,  
303 which was similar to the parent DA (Fig.2). Regarding unexpected products coming from  
304 photodegradation of DA, two peaks appeared significant in irradiated sample compared to control.

305 For each of these peaks, many possibilities of elemental composition were proposed by the software  
306 (Table 2, unexpected products). With i-FIT values linked to a proposed elemental composition for a  
307 given measured mass, from mass error (ppm), retention time (2.54 min.) and assuming impossible  
308 incorporation of more than one nitrogen, the list of proposed elemental composition diminished to  
309 finally go to decarboxylated molecules of DA:  $C_{14}H_{22}NO_4^+$  (m/z 268.1550) and  $C_{14}H_{21}NO_4Na^+$   
310 (m/z 290.1368).

311 Precursor ion informations with fragment analysis  $MS^E$  (MetaboLynx<sup>TM</sup>) gave complete  
312 visualisation of affiliation parent-daughter and daughter-parent ions. Fragment ions combined with  
313 elemental composition searched on spectra allowed to determine the photodegradation products  
314 (Table 3). The software could also give the probability of the position of the transformation by  
315 photodegradation of DA, which allow the structure shown on Figure 6 to be proposed.. Indeed, each  
316 major fragment ions of photodegradation product of DA corresponded to the major fragment ions of  
317 DA with a loss of  $CO_2$  (m/z 43.9898). For confirmation of the decarboxylated of DA, a MS/MS  
318 analysis was realized on m/z 268.15 (Figure 7). All major fragment ions of the decarboxylated  
319 molecule were found. Thus, the algorithm used allowed the detection and identification of unknown  
320 degradation product, after extraction of ion chromatograms for expected transformation products,  
321 based on predicted or unpredicted molecular changes relative to the parent compound DA.

322 This result is in accordance with previous studies, in which exposure of DA to sunlight modified its  
323 chemical structure and produced a suite of isomers (isodomoic acids D, E, or F) and products  
324 tentatively identified as decarboxylated derivatives [28]. More recently, the presence of a DA  
325 photodegradation product corresponding to a decarboxylation product of DA ( $[M+H]^+ = 268$ ) was  
326 observed in seawater matrices, after exposure to a solar simulator [29]. In the same study, it was  
327 shown that high halides concentrations in sea water increased DA photodegradation and altered its  
328 transformation pathway, with the production of a predominant, but unidentified, product ( $[M+H]^+ =$   
329 344). This product was not recovered in the present case.

330 4. Conclusion

331 The proposed UHPLC–ESI- Quadrupole-Time-Of-Flight tandem mass spectrometry MS<sup>E</sup> method  
332 after SPE is a useful tool for the rapid and sensitive detection and structural characterization of DA  
333 from complex samples. UHPLC gives higher separation efficiency and resolution with much lower  
334 solvent consumption than classic HPLC. Q-TOF mass spectrometer allows an unambiguous  
335 identification of researched analytes with exact mass determination and simultaneous quantification  
336 of DA with a LOD equal to 0.75µg L<sup>-1</sup>. Moreover, supplementary post-acquisition treatment can be  
337 performed to find possible DA transformation products, thanks to specific MS<sup>E</sup> acquisition mode of  
338 Q-TOF mass spectrometer. This therefore could be an important tool for routine analysis of DA in  
339 complex matrices and for the environmental monitoring of this toxic substance in the aquatic  
340 environment.

341 Acknowledgements.

342 This study was funded by the CPER “Plateforme Littoral” sub-action “Valorisation  
343 Biotechnologique des ressources marines littorales” and the Programme Opérationnel FEDER  
344 2007-2013, « Compétitivité Régionale et Emploi » Poitou-Charentes.

345

346

347 References

348 [1] T. M. Perl, L. Bédard, T. Kosatsky, J. C. Hockin, E. C. Todd and R. S. Remis, *N. Engl. J. Med.*  
349 **322**, 1775 (1990).

350

351 [2] K. A. Lefebvre and A. Robertson, *Toxicon* **56**, 218 (2010).

352

353 [3] O. M. Pulido, *Mar. Drugs* **6**, 180 (2008).

354

355 [4] K. A. Lefebvre, S. Bargu, T. Kieckhefer and M. W. Silver, *Toxicon* **40**, 971 (2002).

356

357 [5] K. A. Lefebvre, C. L. Powell, M. Busman, G. J. Doucette, P. D. Moeller, J. B. Silver, P. E.  
358 Miller, M. P. Hughes, S. Singaram, M. W. Silver and R. S. Tjeerdema, *Nat. Toxins* **7**, 85 (1999).

359

360 [6] C. A. Scholin, F. Gulland, G. J. Doucette, S. Benson, M. Busman, F. P. Chavez, J. Cordaro, R.  
361 DeLong, A. De Vogelaere, J. Harvey, M. Haulena, K. Lefebvre, T. Lipscomb, S. Loscutoff, L. J.  
362 Lowenstine, R. Marin 3rd, P. E. Miller, W. A. McLellan, P. D. Moeller, C. L. Powell, T. Rowles, P.  
363 Silvagni, M. Silver, T. Spraker, V. Trainer and F. M. Van Dolah, *Nature* **403**, 80 (2000).

364

365 [7] A. Sierra Beltrán, M. Palafox-Uribe, J. Grajales-Montiel, A. Cruz-Villacorta and J. L. Ochoa,  
366 *Toxicon* **35**, 447-453 (1997).

367

368 [8] Y. Ni, K. K. D. Amarasinghe, B. Ksebati and J. Montgomery, *Org. Lett.* **5**, 3771 (2003).

369

370 [9] J. N. Johannessen, *J. AOAC Int.* **83**, 411 (2000).

371

372 [10] R.-C. Bouillon, T. L. Knierim, R. J. Kieber, S. A. Skrabal and J. L. C. Wright, *Limnol.*  
373 *Oceanogr.* **51**, 321 (2006).



374

375 [11] M. A. Quilliam, in: G.M. Hallegraeff and D.M. Anderson, A.D. Cembella (Eds.), Manual on  
376 Harmful Marine Microalgae, Monographs on Oceanographic Methodology, 11, Paris, pp.247  
377 (2003).

378

379 [12] EU, Commission of the European Communities 97/61/CE, Off. J. Eur. Commun. **L295**, 35  
380 (1995).

381

382 [13] Z. Wang, K. L. King, J. S. Ramsdell and G. J. Doucette, J. Chromatogr. A **1163**, 169 (2007).

383

384 [14] Y. He, A. Fekete, G. Chen, M. Harir, L. Zhang, P. Tong and P. Schmitt-Kopplin, J. Agric. Food  
385 Chem. **58**, 11525 (2010).

386

387 [15] L. L. Mafra Jr, C. Léger, S. S. Bates and M. A. Quilliam, J. Chromatogr. A **1216**, 6003 (2009).

388

389 [16] S.S. Bates, A.S.W. de Freitas, J.E. Milley, R. Pocklington, M.A. Quilliam, J.C. Smith and J.  
390 Worms, Can. J. Fish. Aquat. Sci. **48**, 1136 (1991).

391

392 [17] A. Furey, M. Lehane, M. Gillman, P. Fernandez-Puente and K. J. James, J. Chromatogr. A  
393 **938**, 167 (2001).

394

395 [18] E. Barbaro, R. Zangrando, S. Rossi, W. R. Cairns, R. Piazza, F. Corami, C. Barbante and A.  
396 Gambaro, Anal Bioanal Chem. **405**, 9113 (2013).

397

398 [19] Z. Zendong, P. Mccarron Pearse, C. Herrenknecht, M. Sibat, Z. Amzil, R.B. Cole and P. Hess,  
399 J. Chromatogr. A **1416**, 10 (2015).

400 [20] B. K. Matuszewski, M. L. Constanzer, and C. M. Chavez-Eng, Anal. Chem. **75**, 3019(2003)

401

402 [21] O. Pardo, V. Yusà and N. L. A. Pastor, J. Chromatogr. A **1154**, 287 (2007).

403

404 [22] P. R. Costa, R. Rosa, A. Duarte-Silva, V. Brotas and M. A. M. Sampayo, Aquat. Toxicol. **74**, 82  
405 (2005).

406

407 [23] P. Ciminiello, C. Dell'Aversano, E. Fattorusso, M. Forino, G. S. Magno, L. Tartaglione, M. A.  
408 Quilliam, A. Tubaro and R. Poletti, Rapid Commun. Mass SP **19**, 2030 (2005).

409

410 [24] A. López-Rivera, B. A. Suárez-Isla, P. P. Eilers, C. G. Beaudry, S. Hall, M. Fernández Amandi,  
411 A. Furey and K. J. James, *Anal. Bioanal. Chem.* **381**, 1540 (2005).

412

413 [25] P. de la Iglesia, G. Giménez and J. Diogène, *J. Chromatogr. A* **1215**, 116 (2008).

414

415 [26] P. Blay, J. P. M. Hui, J. Chang, J. E. Melanson, *Anal. Bioanal. Chem.* **400**, 577 (2011).

416

417 [27] Y. He, A. Fekete, G. Chen, M. Harir, L. Zhang, P. Tong, P. Schmitt-Kopplin, *J. Agric. Food*  
418 *Chem.* **58**, 11525 (2010).

419

420 [28] R.-C. Bouillon, R.J. Kieber, S.A. Skrabal and J.L.C. Wright, *Mar. Chem.* **110**, 18 (2008).

421

422 [29] K.M. Parkera and W.A. Mitcha, *PNAS* **113**, 5868 (2016).

423

424

425 Table 1. Accurate mass measurements of domoic acid and its major fragment ions.

Elemental composition	Fragmentation/Adduct ion	Theoretical mass m/z	Measured mass m/z	Error (ppm)
$C_{15}H_{22}NO_6Na^+$	$M+H+Na]^+$	334.1266	334.1263	-0.9
$C_{15}H_{22}NO_6^+$	$[M+H]^+$	312.1447	312.1447	0.0
$C_{15}H_{20}NO_5^+$	$[M+H-H_2O]^+$	294.1342	294.1339	-1.0
$C_{14}H_{20}NO_4^+$	$[M+H-CH_2O_2]^+$	266.1392	266.1391	-0.4
$C_{14}H_{18}NO_3^+$	$[M+H-CH_4O_3]^+$	248.1287	248.1283	-1.6
$C_{13}H_{18}NO_2^+$	$[M+H-C_2H_4O_4]^+$	220.1338	220.1335	-1.4
$C_{13}H_{16}NO^+$	$[M+H-C_2H_6O_5]^+$	202.1232	202.1230	-1.0
$C_{12}H_{17}O_2^+$	$[M+H-C_3H_5NO_4]^+$	193.1222	193.1225	+1.5
$C_{12}H_{15}O^+$	$[M+H-C_3H_7NO_4]^+$	175.1123	175.1115	-4.7
$C_{11}H_{13}O^+$	$[M+H-C_4H_9NO_4]^+$	161.0966	161.0965	-0.6

427 Table 2. MetaboLynx analysis of artificial seawater spiked with 0.34 ng/ $\mu$ L versus irradiated  
 428 artificial seawater spiked with 0.34 ng/ $\mu$ L.

Measured mass m/z	Retention time (min)	Area (%)	Elemental composition	Theoretical mass m/z	Error (ppm)	Product Name	i-FIT
<b>Expected products of control artificial seawater</b>							
312.1449	2.21	100	C <sub>15</sub> H <sub>22</sub> NO <sub>6</sub> <sup>+</sup>	312.1447	+0.7	Domoic acid	-
<b>Expected products of irradiated artificial seawater</b>							
312.1449	1.90	6.51	C <sub>15</sub> H <sub>22</sub> NO <sub>6</sub> <sup>+</sup>	312.1447	+0.7	Isodomoic acid	-
312.1449	1.98	13.08	C <sub>15</sub> H <sub>22</sub> NO <sub>6</sub> <sup>+</sup>	312.1447	+0.7	Isodomoic acid	-
312.1447	2.09	10.81	C <sub>15</sub> H <sub>22</sub> NO <sub>6</sub> <sup>+</sup>	312.1447	+0.0	Domoic acid	-
312.1449	2.18	50.54	C <sub>15</sub> H <sub>22</sub> NO <sub>6</sub> <sup>+</sup>	312.1447	+0.7	Isodomoic acid	-
312.1448	2.26	19.06	C <sub>15</sub> H <sub>22</sub> NO <sub>6</sub> <sup>+</sup>	312.1447	+0.4	Isodomoic acid	-
<b>Unexpected products of irradiated artificial seawater</b>							
			C <sub>15</sub> H <sub>18</sub> N <sub>5</sub> <sup>+</sup>	268.1562	-4.5	-	21.6
			C <sub>15</sub> H <sub>21</sub> N <sub>2</sub> ONa <sup>+</sup>	268.1552	-0.7	-	23.3
268.1550	2.54	87.01	C <sub>14</sub> H <sub>22</sub> NO <sub>4</sub> <sup>+</sup>	268.1549	+0.4	Decarboxylated domoic acid	24.1
			C <sub>13</sub> H <sub>19</sub> N <sub>5</sub> Na <sup>+</sup>	268.1538	+4.5	-	25.0
			H <sub>17</sub> N <sub>14</sub> O <sub>2</sub> Na <sup>+</sup>	268.1557	-2.6	-	34.7
			C <sub>14</sub> H <sub>21</sub> NO <sub>4</sub> Na <sup>+</sup>	290.1368	0.0	Decarboxylated domoic acid	9.6
			C <sub>14</sub> H <sub>18</sub> N <sub>4</sub> O <sub>3</sub> <sup>+</sup>	290.1379	-3.8	-	11.0
290.1368	2.54	12.99	C <sub>12</sub> H <sub>16</sub> N <sub>7</sub> O <sub>2</sub> <sup>+</sup>	290.1365	+1.0	-	16.2
			C <sub>15</sub> H <sub>17</sub> N <sub>5</sub> Na <sup>+</sup>	290.1382	-4.8	-	16.3
			C <sub>13</sub> H <sub>22</sub> O <sub>7</sub> <sup>+</sup>	290.1366	+0.7	-	16.6
			C <sub>12</sub> H <sub>19</sub> N <sub>4</sub> O <sub>3</sub> Na <sup>+</sup>	290.1355	+4.5	-	17.4

429 i-FIT: isotopic fit value. The lower the value, the better the fit.

430 Table 3. Accurate mass measurement of decarboxylated domoic acid and its major fragment ions.

<b>Elemental composition</b>	<b>Theoretical mass m/z</b>	<b>Measured mass m/z</b>	<b>Error (ppm)</b>
$C_{14}H_{21}NO_4Na^+$	290.1368	290.1368	+0.0
$C_{14}H_{22}NO_4^+$	268.1549	268.1550	+0.4
$C_{14}H_{20}NO_3^+$	250.1443	250.1445	+0.8
$C_{13}H_{20}NO_2^+$	222.1494	222.1493	-0.5
$C_{13}H_{18}NO^+$	204.1388	204.1388	0.0
$C_{12}H_{18}N^+$	176.1439	176.1440	+0.6
$C_{11}H_{17}^+$	149.1330	149.1325*	-3.4

431 \* Molecular ion found in noise, by eliminating CO<sub>2</sub> molecule from  $C_{12}H_{17}O_2^+$ , the lowest fragment  
432 ion of domoic acid including O<sub>2</sub> (m/z 193.1229).

433

434 Figure Legends

435

436 Figure 1

437 Structure of domoic acid.

438

439 Figure 2

440 Representative profiles mass spectrum with low energy collision in MS<sup>E</sup> mode (parent ion of

441 domoic acid)(A) and mass spectrum with high energy collision in MS<sup>E</sup> mode (fragment ions of

442 domoic acid)(B).

443 Figure 3

444 Possible fragmentation pathway for domoic acid.

445

446 Figure 4

447 Separation of DA and GLF by optimized UHPLC method. DA and GLF Extraction Chromatogram

448 and Total Ion Chromatogram. Compound a corresponds to DA at 2.22 min. Compound b

449 corresponds to GLF at 2.39 min and compounds c, d, e, f, g correspond to plastics pollutants.

450

451

452 Figure 5

453 LC-MS/MS chromatogram after extraction at  $m/z$   $312.14 \pm 0.02$  Da, domoic acid in seawater,

454 before (A) and after (B) UV-irradiation as described in Materials and methods.

455

456 Figure 6

457 Probability of the position of the transformation by photodegradation of domoic acid. Weighted %

458 of the spectral data supporting photodegradation transformation at the position shown.

459

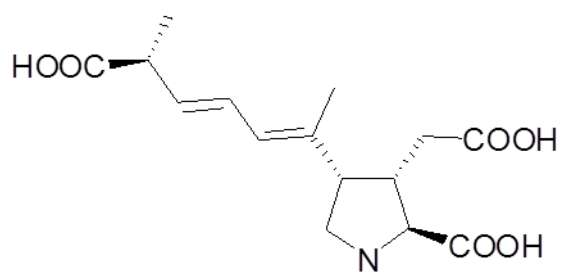
460 Figure7

461 Representative profiles of MS (A) and MS/MS (B) analysis of the decarboxylated domoic acid.

462

463 Figure 1

464



465

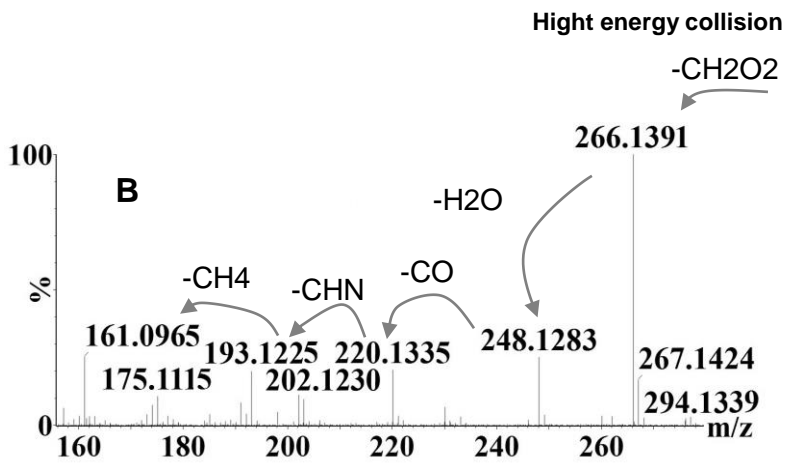
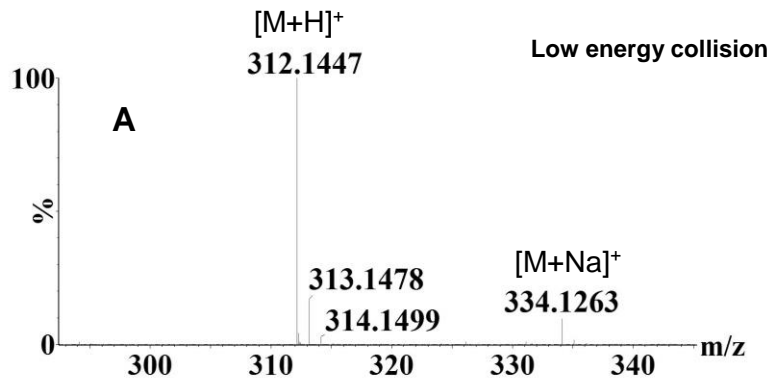
466

467



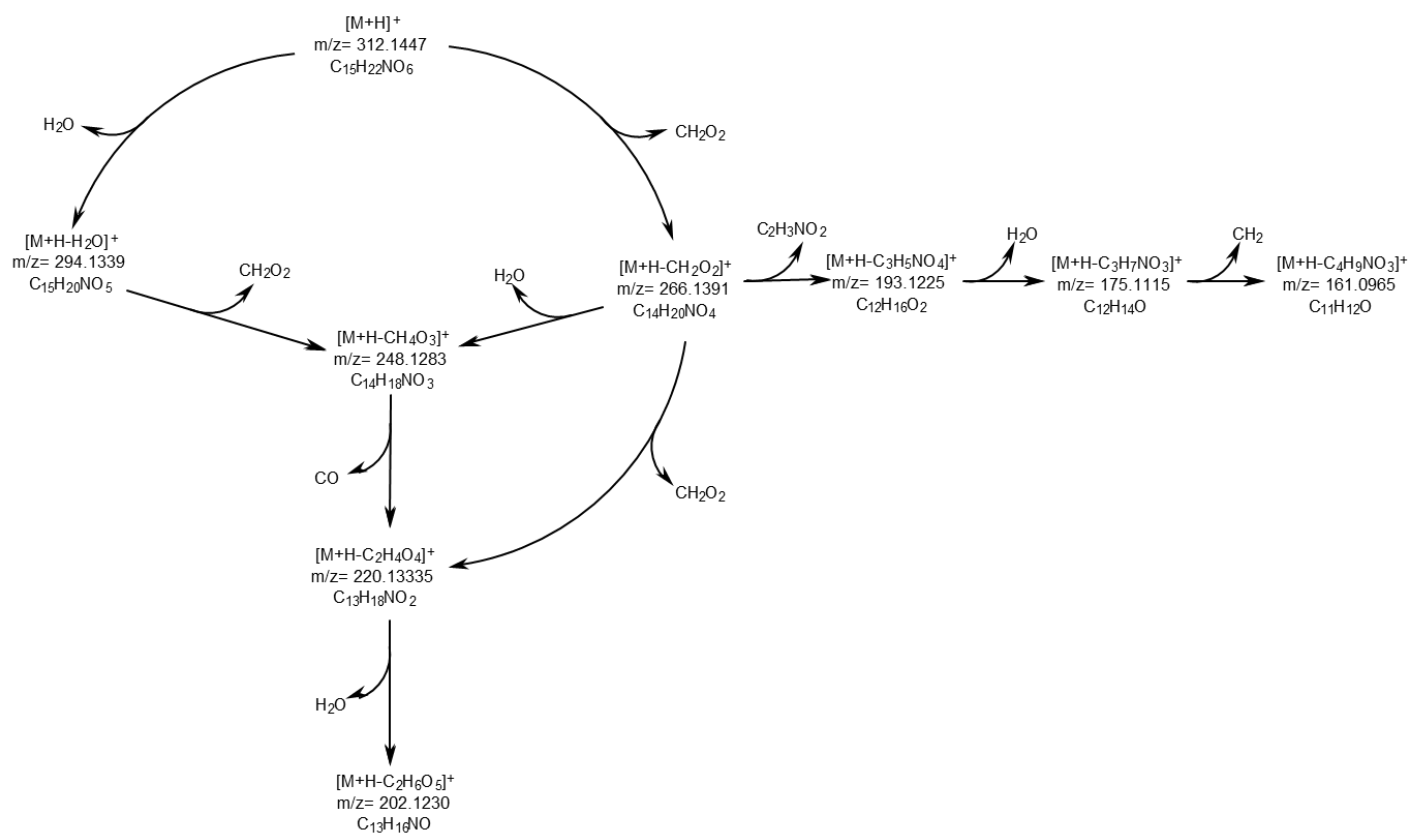
468 Figure 2

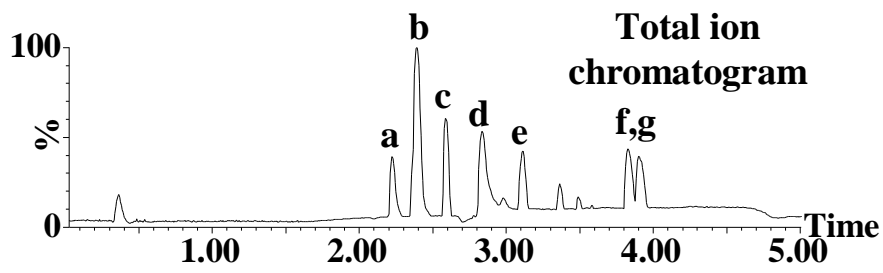
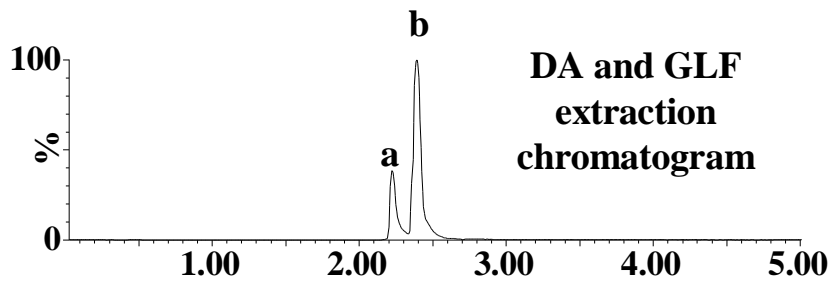
469



470

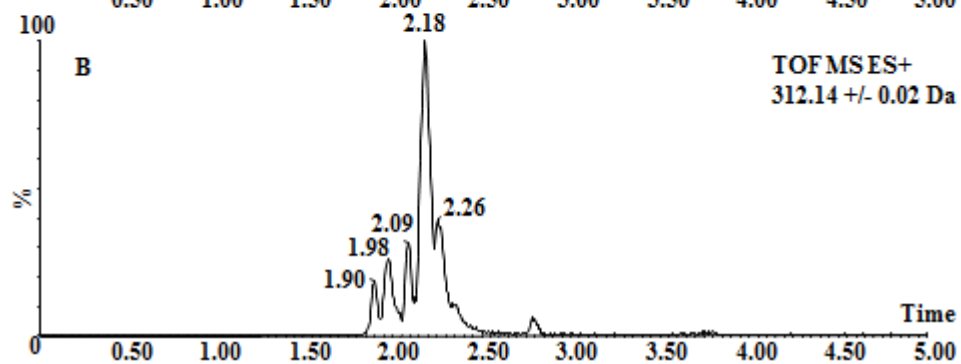
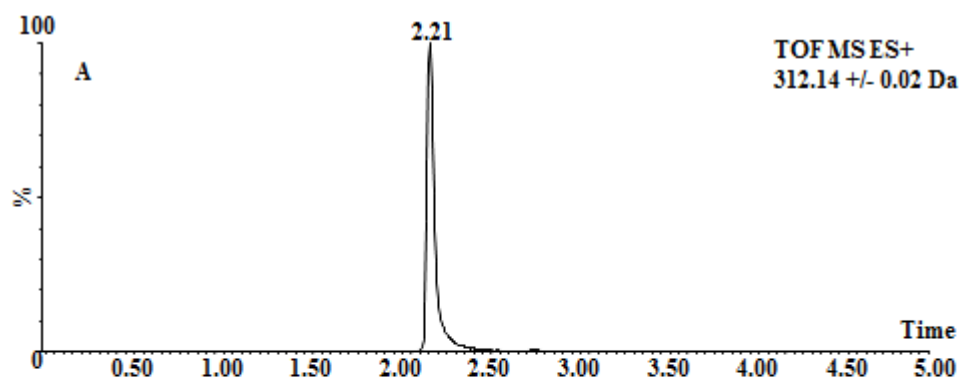
471





477 Figure 5

478

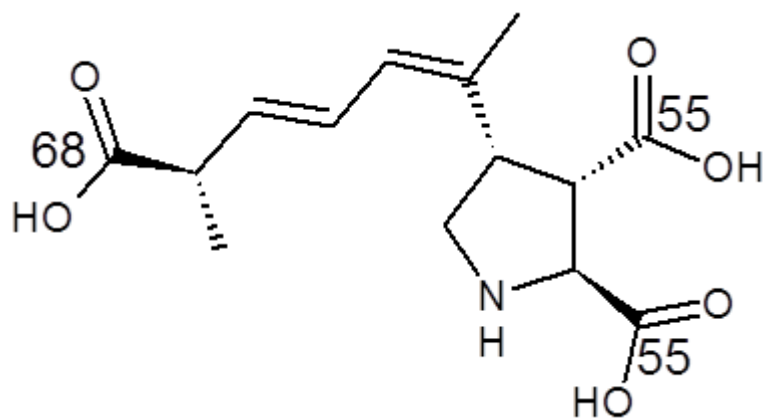


479

480

481

482 Figure 6

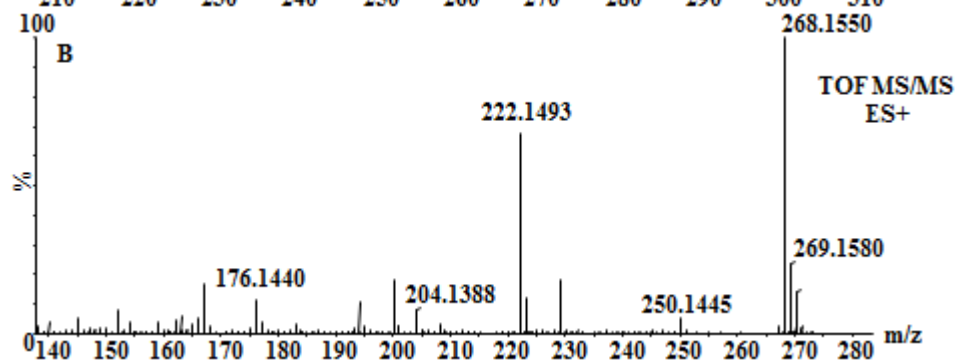
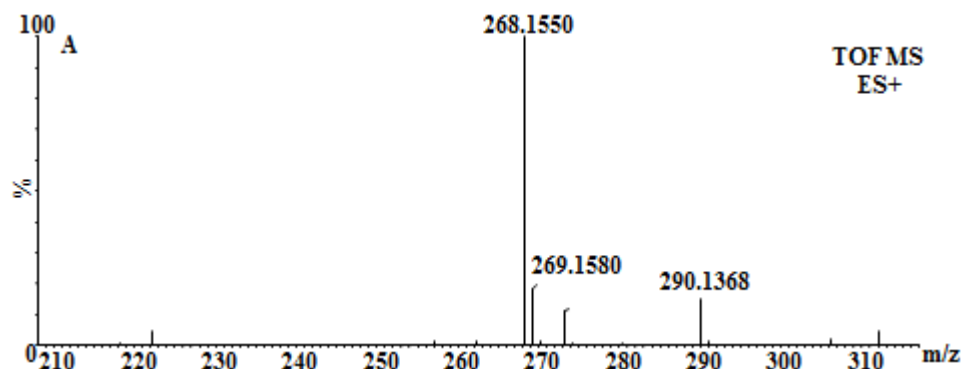


483

484

485

486 Figure 7



487

488